

Valence transition of $\text{Sm}_{1-x}\text{La}_x\text{S}$ and related compounds

Dieter W. Pohl

IBM Zurich Research Laboratory, 8803 Rüschlikon, Switzerland

(Received 16 August 1976)

The pressure-induced semiconductor-metal transition was studied experimentally in $\text{Sm}_{1-x}\text{La}_x\text{S}$ and $\text{Sm}_{1-x}\text{Y}_x\text{S}$. Transition pressure, reflectivity, and lattice compression were measured as a function of composition and hydrostatic pressure. While being strongly first order in Y alloys, the transition in La alloys softens and becomes continuous with increasing concentration. The observed behavior as well as various properties reported in the literature on other alloys can be interpreted in terms of a Falicov-Kimball model. In the theoretical part, we consider the extensions to this model which are to be made to include the effects of alloying. Calculations on the basis of this model agree semiquantitatively with experimental results. In particular, a "universal" critical concentration of $x_{\text{cr}} \simeq 27\%$ is predicted for the changeover from a first-order to a continuous transition independent of the particular type of alloyed cation.

I. INTRODUCTION

The semiconductor-metal transition of SmS with its spectacular change of properties has recently been the subject of extensive research. In particular, the effects of pressure, temperature, and alloying have been investigated in detail.¹⁻⁷

SmS can be readily alloyed with other rare-earth (R) and transition-element sulfides to form compounds of the type $\text{Sm}_{1-x}R_x\text{S}$. The introduction of cations R smaller than Sm^{3+} tends to compress the lattice until at some typical concentration x_{cc} it collapses into the metallic phase.^{4,5} Below x_{cc} the transition can be produced by application of pressure or, close to x_{cc} , by variation of temperature.^{1,4-7} Typical examples for such alloys are $\text{Sm}_{1-x}\text{Y}_x\text{S}$,^{1,5-7} and $\text{Sm}_{1-x}\text{Gd}_x\text{S}$.^{1,4,5} The phase transitions in these compounds are strongly first order and easily recognizable. However, a large hysteresis tends to conceal critical phenomena in these substances. Moreover, after passing the transition once or twice, the samples usually break owing to the associated large lattice contraction. It is difficult, therefore, to get quantitative experimental information on the transition in such alloys.

For this reason, an alloy with intermediate-size cation like $\text{Sm}_{1-x}\text{La}_x\text{S}$ seems more favorable for investigation of the mechanism of the transition. The lattice constant of LaS (5.85 Å) lies in between that of divalent (5.97 Å) semiconducting and trivalent (5.62 Å) metallic SmS.^{2,5} Hence the additional of lanthanum is expected to soften the transition rather than induce it. Hysteresis, lattice contraction, and reflectivity versus pressure were measured and found to support this idea; furthermore, they strongly indicate the existence of a critical point near $x = 0.28$. We also investigated the pressure-induced transition in

$\text{Sm}_{1-x}\text{Y}_x\text{S}$. The results are in agreement with the work of Jayaraman *et al.*¹ Our experimental investigation and results are described in Secs. II and III, respectively.

A number of models, mostly based on the Falicov-Kimball (FK) formalism,⁸ has been proposed to describe valence transitions. It is tempting to compare the experimental data obtained on SmS alloys, in particular $\text{Sm}_{1-x}\text{La}_x\text{S}$, with an appropriately extended FK model.

Such an extension is discussed in Sec. IV which includes the effect of alloying SmS with other sulfides. Introduction of the new variable x (concentration) adds a new dimension to the model which causes a number of interesting situations. It turns out that the transition depends on x far more strongly than, for example, on temperature. The latter will be considered constant throughout this paper. As an important outcome of the present model, a "universal" critical concentration is predicted at which the transition turns over from first order to continuous.

II. EXPERIMENTAL

The $\text{Sm}_{1-x}\text{La}_x\text{S}$ ($x = 3\%, 10\%, 15\%, 20\%$, and 30%) and $\text{Sm}_{1-x}\text{Y}_x\text{S}$ ($x = 7\%, 9\%, 10\%$, and 14%) crystals used in this investigation were prepared by F. Holtzberg at the IBM Thomas J. Watson Research Center, Yorktown Heights. Their basic properties have been described previously.⁵ At ambient conditions, the system SmS-LaS essentially forms a solid solution with a continuous variation of properties between the pure semiconducting SmS and metallic LaS. The Sm ions do not collapse but a slight increase in valence with increasing x is indicated by a nonlinear variation of lattice constant at zero pressure.

Platelets of about $0.3 \times 1 \times 1$ mm in size were

used in the measurements under pressure. They were obtained by cleaving and were carefully polished to allow for reflectivity measurements. Internal stress owing to polishing severely influences the surface properties. The stress was released by means of annealing in nitrogen atmosphere at 220 °C.^{9,10}

The pressure cell was a conventional Bridgman-type apparatus with a maximum pressure of about 7 kbar. A window allowed visual observation of the sample and reflectivity measurements. The variation in linear dimensions of the sample upon application of pressure could be determined with about 0.1% accuracy from photographs of the sample surface.

A Leiss monochromator together with a microscope were used for the reflection spectroscopy. The accuracy of measurement was limited by the small dimensions of the sample and stray light from the pressure cell. Our main emphasis was the observation of the plasma edge and its variation with pressure which could be easily traced between 1.3 and 2.8 eV.

III. RESULTS

A. Visual observation of the phase transition

The phase transition was readily visible using a microscope focused onto the sample in the pressure cell. The well known sudden change in color at the transition was observed for all our La- and Y-doped samples except for $\text{Sm}_{0.7}\text{La}_{0.3}\text{S}$ which has a continuous transition. In Y-doped samples, the transition is abrupt; the samples always breaking into small pieces at the transition back from the metallic to the semiconducting state. Quantitative measurements on these samples except for the transition pressure $p_t(x)$ are difficult to make. In Fig. 1, $p_t(x)$ is plotted; it is in agreement with the description given in Ref. 1.

The transition pressure of $\text{Sm}_{1-x}\text{La}_x\text{S}$, also shown in Fig. 1, differs from the ones above in an interesting way: the lower p_t -vs- x curve (back transformation) seems first to increase ($x < 0.1$) while the upper one remains constant. The latter then strongly decreases and the hysteresis gets very small. We can follow the transition up to $x = 0.2$, where the transformation pressures differ by no more than 0.2 kbar. No first-order transition seems to exist in the sample with the next-higher concentration, $x = 0.3$, at room temperature. This sample changes its properties continuously over a fairly large range of pressures. The strong response is typical for the proximity of a phase transition. The transition curves obviously end in a critical point in between $x = 0.2$ and 0.3.

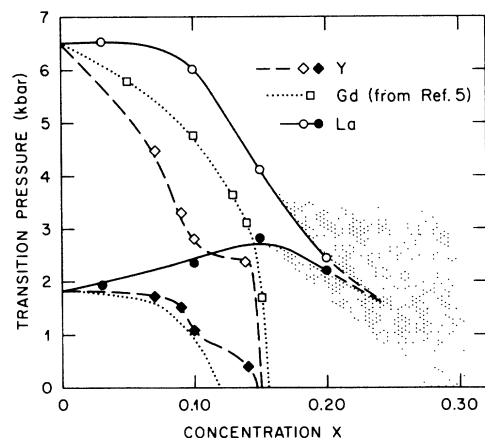


FIG. 1. Experimental transition pressures of $\text{Sm}_{1-x}\text{R}_x\text{S}$ with $R = \text{Y}$, Gd (Ref. 1), and La. The shaded area indicates the range of continuous transition. The curves are guidelines to the eye only.

B. Lattice compression

Lattice compression data are intimately related to the valence of the Sm ions. In Fig. 2(a) the contraction as derived from our measurements has been plotted versus pressure p for $x = 0.10, 0.15, 0.20$, and 0.30. The curve for pure SmS, also shown in Fig. 2(a), is based on the data of Refs. 1, 2, and 11 and our own measurements. The linear contraction at the transition $\delta\Delta$ has been plotted in Fig. 3 together with values for other alloys taken from the literature.^{1,6,12}

C. Reflectivity measurements

An aluminum mirror inserted in the pressure cell was chosen for reference. The reflectivities of different La-alloyed samples with the same x were found to vary considerably, which might be a result of variations in the surface preparation and crystal quality. The variation of the position of the reflectivity edge, however, could be obtained quite reliably. The relative change in reflection close to the plasma frequency ω_p is approximately proportional to $\delta\omega_p/\omega_p \sim 2\delta N_c/N_c$, where N_c is the number of conduction electrons. The shift of the reflectivity edge therefore gives some insight into the change of the Sm valence with pressure. Figure 4 shows the reflectivity edges for $x = 0.15, 0.20$, and 0.30. Crystals with 20% and 30% La do not break even after a large number of pressure cycles; those with $x = 0.15$ tend to break but the fracture pattern remains fairly stable after a few pressure cycles. In these samples, the variation of reflectivity versus pressure can be determined with good reproducibility. The reflection edge is located almost in the visible spectrum for

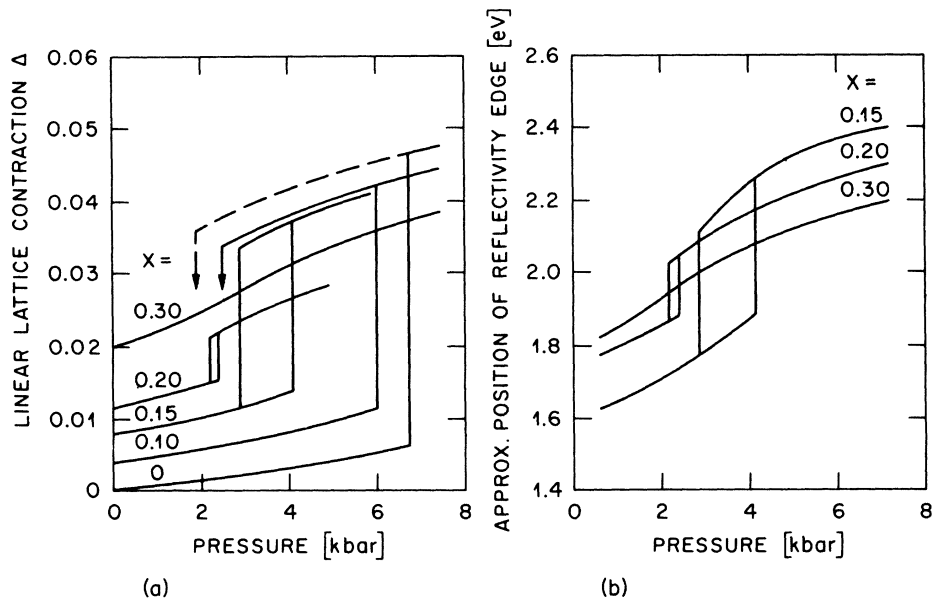


FIG. 2. Experimental lattice contraction (a) and position of reflectivity edge (b) for $\text{Sm}_{1-x}\text{La}_x\text{S}$.

the higher concentrations since each La ion gives one electron to the conduction band. The transitions at 4.1/2.8 kbar for $x = 0.15$ and 2.4/2.2 kbar show up clearly in the reflection spectrum. The reflectivity edge shifts considerably already below the transformation pressure and continues to shift above it. This behavior is typical for the softening of the first-order transition with increasing x . Softening becomes complete at $x = 0.3$. Here, the shift with pressure is continuous for the whole pressure interval; a maximum is seen between 2 and 3 kbar.

The change in character of the transition is summarized in Fig. 2(b), where the frequency of

a characteristic value of reflectivity (35%) close to the reflectivity edge has been plotted. The decreasing hysteresis and the strong pre- and post-transitional variations of reflectivity are clearly visible.

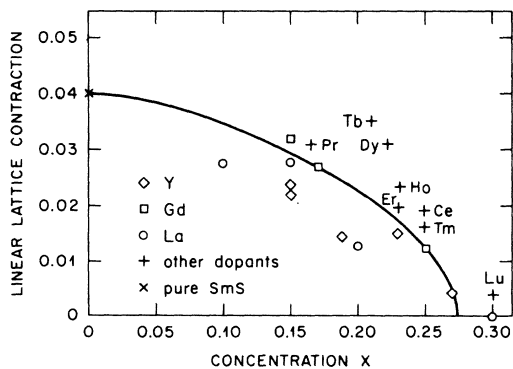


FIG. 3. Experimental and calculated relative linear lattice contractions at the phase transition. Except for the La alloys, the experimental data are taken from Refs. 1, 6, and 12. Solid curve; Eq. (A11).

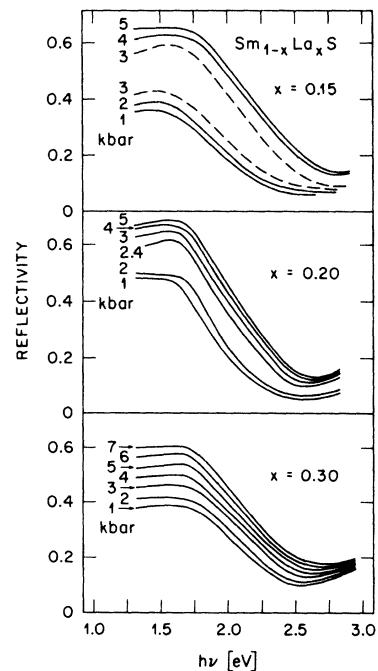


FIG. 4. Reflectivity curves for various pressures. The dashed curves, taken at the same pressure, demonstrate the effect of hysteresis.

IV. THEORY

The model of Falicov and Kimbal⁸ takes into consideration, besides the lattice energy, contributions to the internal energy from the gap between f and d bands, the finite population of the conduction band, and the Coulomb attraction between $4f$ holes and conduction electrons. The occupation number n of holes in the $4f$ levels, variable between 0 and 1, is a characteristic variable for the state of the system; in pure SmS it is equal to the $5d$ -band population. For our analysis, it will be convenient to normalize to equipartition between f and d bands, i.e., to substitute n by $\eta = n - \frac{1}{2}$. The first two contributions to the internal energy only depend linearly on η , while the third and fourth components are essentially quadratic in η . The other characteristic variable is the lattice compression $\Delta = (R - R_0)/R_0$, where R_0 is the distance between Sm^{2+} and S^{2-} in pure SmS at ambient conditions.

The significant contributions to the entropy are of the form $(\eta \pm \frac{1}{2}) \ln(\eta \pm \frac{1}{2})$ and $\eta \ln(Q_M/Q_S)$. The two expressions stand for configuration and spin disorder, respectively; Q_M and Q_S are the spin multiplicities of the metallic and semiconducting phases. All the other contributions do not depend strongly on η and, therefore, are of minor interest here.

The free energy and Gibbs free energy (see below) have minima close to $\eta = \pm \frac{1}{2}$ depending on the sign of the linear term. The latter must be positive for the semiconductor phase and negative for the metal. The transition is continuous if the quadratic term is positive and of first order if it is negative.

Various aspects of the FK model have been considered recently by Falicov and co-workers,¹³ Alascio and co-workers,^{14,15} Bringer,¹⁶ and Avignon and Chatak.¹⁷ Different approaches were made by Adler and Brooks,¹⁸ Hirst,¹⁹ Wohlleben²⁰ and co-workers, Herbst *et al.*,²¹ Sicardi *et al.*,²² and Jefferson.²³ A phenomenological description was given by Varma and Heine for pure SmS.²⁴

In this paper, we shall try to interpret the results on alloys of the type $\text{Sm}_{1-x}\text{R}_x\text{S}$ with particular emphasis on $R = \text{La}, \text{Y},$ and Gd . For this purpose, we restrict ourselves to a simple form of the above model neglecting, for example, the effect of hybridization between f and d electrons,^{16,17} or interconfiguration fluctuations.^{19,20} In the derivation of the results we shall follow, to a certain extent, the analysis of Alascio, Lopez, and Wio.¹⁵

Doping of SmS with RS influences the properties of the intrinsic material in a threefold way: lattice compression, band-gap shift, and conduction-band population change (for trivalent cations).

The stability of a system at a given pressure depends on the Gibbs free energy G rather than on the free energy. G is given by the well-known combination of internal energy U , entropy S , and volume V (per ion):

$$G = U - TS + pV. \quad (1)$$

Both U and S depend on composition x in addition to the variables necessary to describe pure SmS, viz., temperature T , pressure p , occupation number η , and lattice compression Δ . The values of η and Δ can be derived from the minimum condition for G if explicit expressions for U and S are known. For this purpose, the following simplifying assumptions are made:

(i) Rigid lattice and linear superposition of potentials U_L^i ($i = \text{Sm}, \text{R}$):

$$U_L(\Delta) = (1-x)U_L^{\text{Sm}}(\Delta) + xU_L^{\text{R}}(\Delta). \quad (2)$$

(ii) Quadratic approximation for U_L^i :

$$U_L^i = 6R_0^3 p_1(\Delta_0^i)(\Delta - \Delta_0^i)^2. \quad (3)$$

$2R_0^3$ is the volume per ion pair (NaCl structure). p_1 equals 3 times the bulk modulus. The latter increases considerably when going from divalent to trivalent compounds^{11,25} and varies in a systematic way with lattice constant.²⁴ p_1 in Eq. (3), therefore, is assumed to depend on Δ_0^i , the minimum position of $U_L^i(\Delta)$. Note that, in general, $\Delta \neq \Delta_0^i$ since Δ adjusts to the minimum of G . Δ_0^i is determined from the lattice constants of Sm^{2+}S , Sm^{3+}S , and RS , respectively (Table I). For the mixed-valent state, we put $\Delta_0^{\text{Sm}} = n\alpha$ with $\alpha = 0.059$.¹⁵

(iii) The electronic energy U_e consists of three parts:

$$U_e = \epsilon_c N_c + (1-x)(n\bar{\Delta} - \bar{G}N_c n). \quad (4)$$

ϵ_c is the one-particle energy in the conduction band $\approx \bar{B}N_c$.¹⁴ $N_c = (1-x)n + x$ is the total number of conduction electrons. $\bar{\Delta}$ is the gap between localized and band states. \bar{G} accounts for the

TABLE I. Lattice-constant shift Δ_0^i , bulk modulus $\frac{1}{3}p_1^{(i)}$, and lattice pressure $p_1^{(i)}$ for Sm^{3+}S and RS .

Cation	Δ_0^i	$\frac{1}{3}p_1^{(i)}$	p_1
			(kbar)
Sm^{2+}	0	476 ^a	...
Sm^{3+}	0.059	900	...
Y	0.079	1000 ^b	240
Gd	0.070	950	200
La	0.020	740	45
Nd	0.040	815	100
Yb	0.039	730 ^c	86

^aReference 9.

^bReference 25.

^cReference 11.

Coulomb attraction between $4f$ holes and conduction electrons. The difference between \bar{B} and \bar{G} is important for the character of the transition.

(iv) The gap $\bar{\Delta}$ depends linearly on lattice compression and concentration:

$$\bar{\Delta} = \bar{\Delta}_0 + x(\partial\bar{\Delta}/\partial x) - \gamma R_0 \Delta, \quad (5)$$

with $\bar{\Delta}_0 = 0.1 - 0.2$ eV.²

Doping with three-valent ions will tend to reduce the gap, $\partial\bar{\Delta}/\partial x < 0$, while doping with divalent Yb, for instance, will make this quantity strongly positive.

The expression for the entropy may be written as a sum of band (S_B), spin (S_S^{sm}), and configuration (S_C^{sm}) disorder.^{8,15} The disorder in the arrangement of Sm and R cations is frozen in and hence does not depend on η . It is also assumed that S does not depend directly on Δ .¹⁵ The only contributions of interest are terms which contain η :

$$S = S_B(s, \eta) + (1-x)[S_S^{\text{sm}}(\eta) + S_C^{\text{sm}}(\eta)]. \quad (6)$$

G is next expanded around its equilibrium value for $x = \Delta = n = 0$, i.e., pure SmS at ambient conditions. (The temperature will be considered constant.) The resultant expression for the Gibbs free energy gains transparency from the introduction of a number of "pressures" defined in Table II.

Configurational (Ref. 15), lattice, and electronic pressures are given, respectively, by

$$p_0^{(2,3)} = \alpha p_1^{(2,3)} + \gamma/12R_0^2, \quad (7)$$

$$p_l = \Delta^R p_l^R, \quad (8)$$

$$p_e = -(\dot{p}_0^{(3)}/p_{1av})(\bar{B} + \partial\bar{\Delta}/\partial x)/6R_0^3. \quad (9)$$

Alascio *et al.*¹⁵ estimate $p_0^{(2)} \approx 100-150$ kbar which yields $p_0^{(3)} \approx 130-180$ kbar.

A few values for $\frac{1}{3}p_1^{(4)}$ and p_l are given in Table I. $p_1^{(3)}$ and p_1^R have been calculated from the value for YS,²⁵ using the empirical relation discussed in Refs. 11 and 24. p_e cannot easily be determined

TABLE II. Definition of pressures used in the text.

Designation	"Pressures" referring to		
	Sm^{2+}S	Sm^{3+}S	RS
"3 times bulk modulus"	$p_1^{(2)}$	$p_1^{(3)}$	p_1^R
-average		p_{1av}	...
-differences	...	Δp_1^{sm}	Δp_1^R
"configurational p "	$p_0^{(2)}$	$p_0^{(3)}$...
-average		p_{0av}	...
"chemical p "	$p_c = p_l + p_e$
-lattice	p_l
-electrons	p_e

with the present incomplete knowledge on the band structure of rare-earth chalcogenides.

The minimum condition $\partial G/\partial \Delta = 0$ yields the equilibrium compression $\Delta(\eta)$ in terms of pressures

$$\Delta_{\text{eq}} = [p + xp_c + (1-x)(\frac{1}{2}p_{0av} + \eta p_0^{(3)} + \eta^2 \Delta p_1^{\text{sm}})]/p_{1av} \times f(x, \eta, \Delta p_1^R), \quad (10)$$

where f is a weak function of its three arguments (Appendix A). As to be expected, the effect of chemical pressure goes parallel to that of external pressure p ; the effect of d -band population ($\eta \rightarrow +\frac{1}{2}$) increases the compression. Δ_{eq} vanishes for $x = p = 0$, $\eta = -\frac{1}{2}$.

Bearing in mind Eq. (16), the free enthalpy is written as a function of η only:

$$G \approx G_0(x) + (1-x)(G_1\eta + G_2\eta^2 + G_4\eta^4), \quad (11)$$

with the expansion coefficients

$$G_1 = F_{10}(T) - g[p + x(p_c - \frac{1}{2}p_{0av})], \quad (12)$$

$$G_2 = F_{20}(T) + (1-x)F_{21}(T), \quad (13)$$

$$G_4 = \text{const.} \quad (14)$$

The less important expressions for the coefficients F_{10} , g , F_{20} , and F_{21} are given in Appendix A. F_{10} , g , and F_{20} are independent of the properties of R. F_{21} is a very weak function of p_1^R . For this reason, all the coefficients can be determined with fair accuracy from the data of pure SmS.

The third-order term in the expansion of G was estimated to be small and has been omitted. G_4 is required in order to allow for mixed-valent states. In view of insufficient experimental data, however, we refrain from presenting an analytical expression for G_4 .

V. DISCUSSION

Equation (11) has the well-known Landau form including a term of first order in η . The type of transition—which should be either first order or continuous according to experimental experience—depends on the sign of G_2 . The first-order transition of pure SmS requires $G_2(0) = F_{20} + F_{21} < 0$. Equation (A3) shows that $F_{20} > 0$; hence $F_{21} < 0$. There is a critical concentration x_{cr} where G_2 changes sign:

$$x_{\text{cr}} = (F_{20} + F_{21})/F_{21}. \quad (15)$$

The transition is first order for $x < x_{\text{cr}}$ and continuous for $x > x_{\text{cr}}$. A rough estimate using Eqs. (A2) and (A3) yields $x_{\text{cr}} \approx (20 \text{ to } 35)\%$. The exact value of x_{cr} should not differ much from alloy to alloy.

This result agrees well with our experimental data on $\text{Sm}_{1-x}\text{La}_x\text{S}$. A careful survey of the liter-

ature data^{1,6,12} moreover reveals that indeed no first-order transition has ever been found above $x = 0.3$. Jayaraman *et al.*¹ recently investigated the temperature-induced transition in $\text{Sm}_{1-x}\text{Gd}_x\text{S}$ and also came to the conclusion that critical points might exist for this alloy close to 30%.

Closely related to the existence of a critical point is the "softening" of the first-order transition with increasing x . The lattice contraction $\delta\Delta$ at the transition may serve as a measure of the softening.

Equation (10) yields an expression of the form

$$\delta\Delta = \delta\eta(x)(a_0 + a_1x + a_2x^2), \quad (16)$$

with

$$\delta\eta(x) = \delta\eta(0)(1 - x/x_{cr})^{1/2}. \quad (16a)$$

$\delta\eta(x)$ is the distance of the free enthalpy minima at the transition, with the experimentally well-established value of $\delta\eta(0) = 0.7$. The coefficients a_0 , a_1 , and a_2 can be estimated with fair accuracy from the known values of $p_1^{(i)}$ and estimates of p_c and $p_0^{(2)}$, $p_0^{(3)}$. a_1 and a_2 slightly depend on the properties of R [Appendix A, in particular Eq. (A11)].

Equation (16) is to be compared with the experimental lattice contraction plotted in Fig. 3. The decay of all the experimental data towards $x \approx 0.27$ is quite obvious.

The solid curve is obtained from Eq. (A11) equal to Eq. (16) which may be considered representative for the average effect of alloying. Note the good agreement at $x = 0$. Scattering of the experimental points for $0 < x < x_{cr}$ may be the result of the different "electronic pressure" which has been neglected here. The data, e.g., for Tb, Dy, Ho, Er, and Tm can be well fitted to Eq. (16) with somewhat larger p_c 's. It should also be noted that some of the experimental points refer to measurements at temperatures different from ambient.

With regard to the transition pressure $p_t(x)$ we shall ignore the experimental hysteresis. Being strongly influenced by G_4 it cannot be treated adequately within the framework of the present model. The limit of stability is reached when the minima of G are at equal height requiring (since we neglect third-order terms) $G_1(x, p) = 0$. Equation (12) yields

$$p_t(x) = p_t(0) + x(\frac{1}{2}p_0 - p_c), \quad (17)$$

where $p_t(0) \approx 4$ kbar is the approximate average of the experimental values for the transition in both directions in pure SmS.

The transition pressure will decrease if $p_c > \frac{1}{2}p_0$. The experimental transition-pressure curves shown in Fig. 1 indicate that this condition is satisfied for $R = \text{Y}$, Gd, and, marginally, La. For Y

and Gd doping (and many other rare earths)¹ the effect of chemical pressure is so strong that p_t becomes zero far below x_{cr} . The condition for "chemical collapsing" is

$$x_{cc} = p_t(0)/(p_c - \frac{1}{2}p_0). \quad (18)$$

In $\text{Sm}_{1-x}\text{La}_x\text{S}$ the transition pressure remains positive at x_{cr} . The extrapolated value at the critical point is close to 2 kbar. Critical exponents should be measurable in this alloy and help to fully parametrize the equation of state (11). (Samples with the appropriate concentration were, unfortunately, not available.)

The lattice contraction $\Delta(p=0)$ at ambient conditions and its relation to the intermediate valence has been discussed by several authors.^{1,2,5,6} It should be mentioned here for completeness that $\Delta(p=0)$ is also given by Eq. (10).

The situation of $\text{Sm}_{0.7}\text{La}_{0.3}\text{S}$ deserves particular consideration being the only case of a pressure-induced transition beyond the critical point.

The experimental lattice compression yields the remarkably small bulk modulus of 120 kbar (cf. Table I in Ref. 11). Similarly small values have been found for $\text{Sm}_{1-x}\text{Y}_x\text{S}$ in the collapsed phase with $x = 0.25$ and 0.28 .²⁵ The latter result fits well to our model which predicts a negative critical pressure for Y alloys. At $p = 0$ the system is then still pretty close to criticality and, therefore, very susceptible to variations in external pressure.

VI. CONCLUSION

The extended Falicov-Kimball model as discussed in Sec. IV seems to be well suited for a semiquantitative description of $\text{Sm}_{1-x}\text{R}_x\text{S}$ alloys. In particular, it predicts a "universal" critical concentration where the transition becomes continuous. The experimental results on $\text{Sm}_{1-x}\text{La}_x\text{S}$ and other alloys support this finding.

For further studies the model can be extended in various ways: mathematically, by inclusion of third-order terms and better expansions for the potentials and entropies; physically, by better assumptions on the lattice potential and its variation with x , by allowing for lattice parameter variations in the neighborhood of R ions, by consideration of hybrid electronic states, etc.

On the experimental side, more detailed knowledge on the band structure (for the calculation of p_e) and on the properties of the pure compounds RS would be desirable. Investigations close to the critical concentration are important.

In the present work, the semiconductor-metal transition has been treated completely within the framework of the classical Landau theory. The same is true for all the other approaches based on

the FK model. Because of the importance of strain, the driving forces have long-range character. The behavior, therefore, near the critical point is indeed expected to be of the mean-field Landau-type calculated here. Similar behavior has recently been observed by Parks²⁶ in the mixed-valence system $\text{Ce}_{1-x}\text{Th}_x$.

Experimental investigations of the critical behavior of the SmS system have, so far, been impeded by the strong first-order character of the transition. The large hysteresis between the two transition pressures has not only prevented the approach to the critical regime, but also physically destroyed the samples. The softening of the transition observed in $\text{Sm}_{1-x}\text{La}_x\text{S}$ may lead to a way out of this dilemma.

Recently, the author became aware of related work on SmS-YS and SmS-SmAs by T. Penney and R. L. Melcher, (IBM Research Report RC 6120, to be published). The authors made a similar *ansatz* for the lattice potential. However, they neither consider the Coulomb attraction between d electrons and f holes, nor the one-particle energy in the d band, i.e., the quadratic contributions to the electronic energy. In the present model, these quantities are essential for the existence and position of the critical point.

ACKNOWLEDGMENTS

The author wishes to thank F. Holtzberg for providing the $\text{Sm}_{1-x}\text{La}_x\text{S}$ and $\text{Sm}_{1-x}\text{Y}_x\text{S}$ crystals. He is also indebted to K. Gisler for skillful technical assistance. Stimulating discussions with K. A. Müller and E. Courtens were of benefit to the present work.

APPENDIX A

1. Expressions for coefficients of Δ_{eq} and G

The various pressures defined in Table II and Eqs. (7)–(9) enter as lengthy combinations the ex-

pressions for Δ_{eq} and G . The explicit forms of f , F_{10} , g , F_{20} , and F_{21} in Eqs. (10), (12), and (13) are

$$f(x, \eta, \Delta p_1^R) = 1 + [x(\Delta p_1^R - \frac{1}{2}\Delta p_1) + (1-x)\Delta p_1\eta]/p_{1av}, \quad (\text{A1})$$

$$g = 6R_0^3 p_0^{(3)}/p_{1av} \quad (\text{A2a})$$

$$F_{10} \approx \frac{1}{2}g p_{0av} + kT(1 + 2x - \ln 2) + (\bar{\Delta}_0 + \bar{B} - \bar{G}), \quad (\text{A2b})$$

$$F_{20} = 3\alpha^2 R_0^3 (p_1^{(3)} + \frac{1}{2}\Delta p_1) + kT, \quad (\text{A3})$$

$$F_{21} = -3(1 - \epsilon x)R_0^3 (p_0^{(3)})^2/p_{1av} + (\bar{B} - \bar{G}). \quad (\text{A4})$$

F_{21} is a weak function of x and Δp_1^R through

$$\epsilon = (\Delta p_1^R - \Delta p_1/2)/p_{1av} \approx \frac{1}{3} \text{ to } \frac{1}{4}. \quad (\text{A5})$$

2. Lattice contraction at the transition

Assume $\eta(\text{before}) = -\eta(\text{after})$ as required by Eq. (11). Neglecting several small terms and expanding the denominator in Eq. (10) [see (A1)], yields

$$\delta\Delta = \delta\eta[RQ_2 - Q_1S - \frac{1}{4}S^2\delta\eta^2(0)] \times (1 - x\Delta p_1/p_{1av})/(p_{1av})^2, \quad (\text{A6})$$

with the abbreviations

$$Q_1 = p + xp_c + \frac{1}{2}(1-x)p_0, \quad (\text{A7})$$

$$Q_2 = (1-x)p_0^{(3)}, \quad (\text{A8})$$

$$R = p_{1av} + x(\Delta p_1^R - \frac{1}{2}\Delta p_1), \quad (\text{A9})$$

$$S = (1-x)\Delta p_1. \quad (\text{A10})$$

Introduction of the known values of the pressures $p_1^{(4)}$ (Table I), of $\delta\eta(0)$ as well as the estimated values of $p_0^{(2)}$ and $p_0^{(3)}$, and putting for simplicity $p_c \approx p_t$ (some average value) yields

$$\delta\Delta = (0.04 + 0.056x - 0.21x^2)(1 - x/x_{cr})^{1/2}. \quad (\text{A11})$$

(A11) has been plotted in Fig. 3.

¹A. Jayaraman, P. Dernier, and L. D. Longinotti, Phys. Rev. B **11**, 2783 (1975).

²B. Batlogg, E. Kaldis, A. Schlegel, and P. Wachter, Phys. Rev. B **14**, 5503 (1976).

³Fairly complete lists of references may be found in Refs. 1 and 2 and in the review article of C. M. Varma, Rev. Mod. Phys. **48**, 219 (1976).

⁴A. Jayaraman, E. Bucher, P. D. Dernier, and L. D. Longinotti, Phys. Rev. Lett. **31**, 700 (1973).

⁵F. Holtzberg, AIP Conf. Proc. **18**, 478 (1973).

⁶L. J. Tao and F. Holtzberg, Phys. Rev. **11**, 3842 (1975); G. Güntherodt and F. Holtzberg, Solid State Commun. **18**, 181 (1976).

⁷T. Penney and F. Holtzberg, Phys. Rev. Lett. **34**, 322.

⁸L. M. Falicov and J. C. Kimball, Phys. Rev. Lett. **22**, 997 (1969).

⁹E. Kaldis and P. Wachter, Solid State Commun. **11**, 907 (1972).

¹⁰D. W. Pohl, R. Jaggi, K. Gisler, and H. Weibel, Solid State Commun. **17**, 705 (1975).

¹¹A. Jayaraman, A. K. Singh, A. Chatterjee, and S. Usha Devi, Phys. Rev. B **9**, 2513 (1974).

¹²M. Gronau and S. Methfessel (private communication).

¹³R. Ramirez, L. M. Falicov, and J. C. Kimball, Phys. Rev. B **2**, 3383 (1970); C. E. J. Conçalves da Silva and L. M. Falicov, J. Phys. C **5**, 906 (1972); Solid State Commun. **17**, 1521 (1975).

¹⁴B. Alascio, V. Grünfeld, and A. Lopez, Phys. Rev.

- B 5, 3708 (1972).
- ¹⁵B. Alascio and A. Lopez, *Solid State Commun.* 14, 321 (1974); H. S. Wio, B. Alascio, and A. Lopez, *Solid State Commun.* 15, 1933 (1974).
- ¹⁶A. Bringer, *Z. Phys. B* 21, 21 (1975); *J. Magn. Magnetic Mater.* (to be published).
- ¹⁷M. Avignon and S. K. Ghatak, *Solid State Commun.* 16, 1243 (1975).
- ¹⁸D. Adler and H. Brooks, *Phys. Rev.* 155, 826 (1967).
- ¹⁹L. L. Hirst, *J. Phys. Chem. Solids* 35, 1285 (1974).
- ²⁰M. B. Maple and D. Wohlleben, *Phys. Rev. Lett.* 27, 511 (1971); B. C. Sales and D. Wohlleben, *Phys. Rev. Lett.* 35, 1240 (1975).
- ²¹J. F. Herbst, R. E. Watson, and J. W. Wilkins, *Solid State Commun.* 13, 1771 (1973).
- ²²J. R. I. Sicardi, A. K. Bhattacharjee, R. Jullien, and B. Coqblin, *Solid State Commun.* 16, 499 (1975).
- ²³J. H. Jefferson, *Phys. Lett. A* 54, 203 (1975).
- ²⁴C. M. Varma and V. Heine, *Phys. Rev. B* 11, 4763 (1975).
- ²⁵T. Penney, R. L. Melcher, F. Holtzberg, and G. Güntherodt, *AIP Conf. Proc.* (to be published).
- ²⁶R. D. Parks, *J. Phys. (Paris)* (to be published).

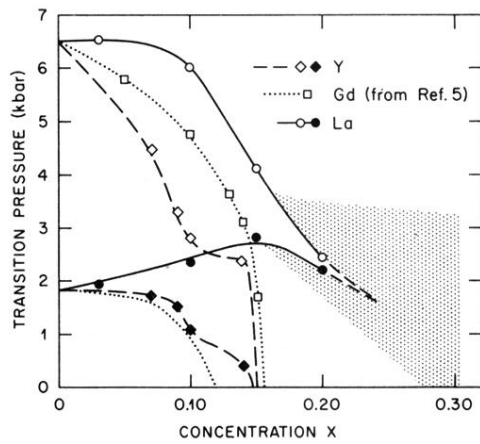


FIG. 1. Experimental transition pressures of $\text{Sm}_{1-x}\text{R}_x\text{S}$ with $R = \text{Y}$, Gd (Ref. 1), and La. The shaded area indicates the range of continuous transition. The curves are guidelines to the eye only.